

Simulation of microwave scattering in Doppler reflectometry experiment

V.V.Bulanin, E.Z.Gusakov*, A.V.Petrov, M.V.Yefanov

St.Petersburg State Technical University, St.Petersburg, 195251, Russia

**Ioffe Institute, St.Petersburg, 194021, Russia*

Shear of plasma rotation is believed to be a key factor of turbulence suppression and transport barrier formation in the fusion devices. The Doppler reflectometry has recently been employed for localized measurements of poloidal velocity in toroidal devices [1]-[4]. The method is based on evaluation of rotation velocity from the Doppler frequency shift of back-scattering radiation that is expected under microwave oblique incidence onto cutoff surface. The possibility to achieve high spatial and k-resolution under the oblique incidence was first mentioned in the 2D theoretical analysis performed in the linear approximation for O-mode microwave propagation [5]. The comprehensive full-wave approach to Doppler reflectometry modelling in slab geometry has been developed afterwards for specific condition of experiment in the W7-AS stellarator [4]. The performance of O-mode Doppler reflectometry is numerically investigated in the present paper in view of realistic microwave beam divergence and a finite curvature of cutoff layer.

An approach to numerical integration

The 2D numerical integration is based on the relation that links the electric field of scattered radiation directly in receiving waveguide and plasma density fluctuations $\delta n(\mathbf{r},t)$ for arbitrary spatial distribution of background index of refraction [6]. The relation obtained in the Born approximation with use of the antenna or receptivity theorem allows to express beat signal of microwave mixer for the O-mode propagation

$$I(t) = \frac{\eta}{8\pi} \int \frac{\delta n(\mathbf{r}, t)}{n_c} W(\mathbf{r}) d^2 r \quad (1)$$

where η is a dimensional constant, n_c is the cut-off density, $W(\mathbf{r}) = E_i(\mathbf{r})E_a(\mathbf{r})$ is the complex spatial weighting function with the real and imaginary parts determining sine and cosine signals of a quadrature detector. $E_i(\mathbf{r})$ is amplitude of unperturbed electric field of probing beam in scattering volume, and $E_a(\mathbf{r})$ is imaginary electric field of radiation that is launched into the plasma via the receiving antenna. Being calculated, the weighting function allows to evaluate the detector response for any shape of fluctuations. To compute the weighting function the electric fields have been calculated for stratified and axially symmetric

distributions of background plasma density - $n(x)$ or $n(r)$. In a case of slab geometry the microwave beams at plasma boundary have been described by the linear superposition of plane waves. Angular spectrum of these waves was determined by the field distribution near antenna mouth. The field distribution along the inhomogeneity direction in plasma was calculated by a one-dimensional wave equation. Similarly the field distribution has been found in axially symmetrical case. The beams were represented as the superposition of cylindrical waves. Their radial dependence in free space was determined by the Hankel functions. After numerical computation of the electric fields the weighting functions $W(x,y)$ and $W(r,\theta)$ were expressed by a 2D matrix product.

Results of simulation

Most of computations were carried out for the microwave scheme with monostatic antenna, which is used, both for probing, and for receiving of scattered signal, that is for $|E_i(\mathbf{r})| = |E_a(\mathbf{r})|$. In optics representation it means that the antenna receives the refraction order -1 [4]. To investigate an influence of the antenna beam divergence on the spatial and wave number resolutions the calculations have been performed for gradient region of the ITER-like device. Fig.1a shows an example of computation for tilt angle $\alpha = 20^\circ$ and incident beam frequency $F = 60\text{GHz}$. The weighting function pattern is exhibited here as a 2D plot for the case of the probing Gaussian beam with radius $w_0 = 4\text{cm}$. In figure it is clearly seen, that the scattering will be mainly observed from fluctuations well localized in radial direction along which the velocity of poloidal rotation is expected to be dramatically changed during the L-H transition. Moreover, the volume of enhanced scattering is elongated in poloidal direction that can be evidently seen on the weighting function pattern represented in the $r-\theta$ frame (see Fig.1b). So the method yields a high selectivity with respect to poloidal wave number. To verify these statements the detector response has been calculated

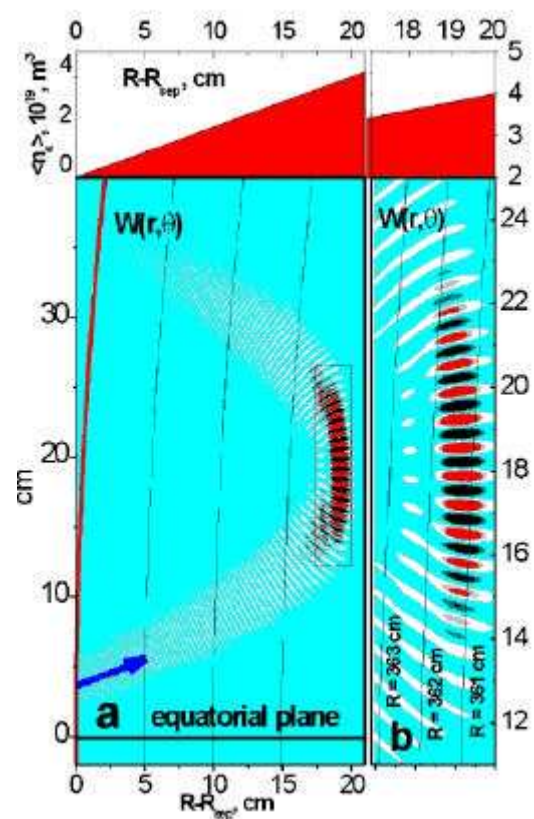


Fig.1 (a) Weighting function $W(R-R_{sep}, \theta)$ for $\alpha=20^\circ$, $F=60\text{GHz}$, $w_0 = 4\text{cm}$ computed for a density profile shown above. The direction of incident beam is marked by blue arrow. Read curve shows a separatrix, $R_{sep}=3.3\text{ m}$. (b) The same function in the $\{R- R_{sep}, \theta\}$ frame.

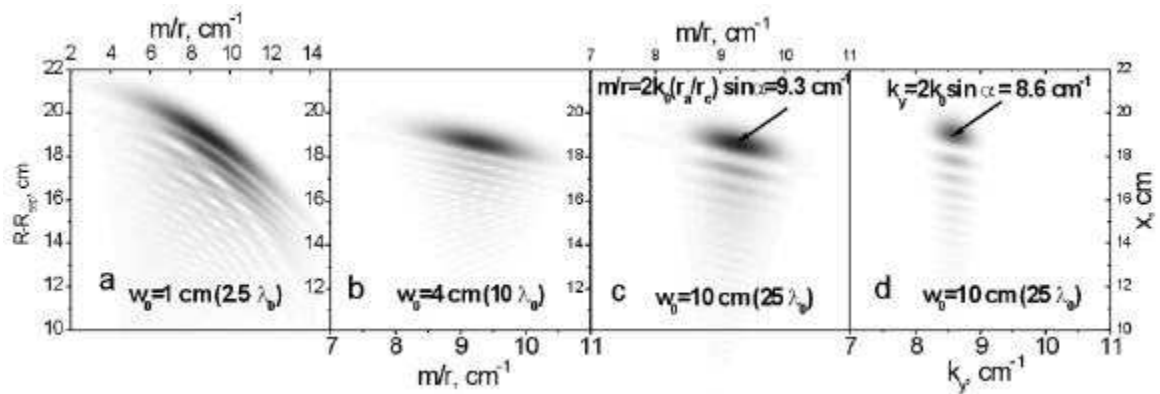


Fig.2 Module of detector response versus poloidal wave number and radial position of scattering fluctuations layer ($w_r=w_x=0.2$ cm). (c) and (d) Comparison between cylindrical and slab models. Arrows mark the mean k -values calculated for slab and cylindrical cases. r_a is radial position of antenna, r_c is radius of beam trajectory turn point.

with the use of formula (2) for scattering from testing fluctuations in a form of radially localized poloidal waves

$$\delta n(r, \theta) = \delta n_0 \exp[(r - r_0)^2/w_r^2] \cos(m\theta); \quad \delta n(x, y) = \delta n_0 \exp[(x - x_0)^2/w_x^2] \cos(k_y y) \quad (4)$$

The 2D plots of the detector response as function of poloidal wave number and radial position of layer (r_0 or x_0) are compared on Fig.2 for various radii of microwave beams. Strictly speaking the wave vector of scattering fluctuations along the trace of microwave beam is not purely poloidal and is a mix of the both poloidal and radial components. To understand how the scattering from fluctuation with different wave vector to contribute to detector response, a maximum of the weighting function module was computed as a function of plasma radius at various antenna divergences. This dependence for slab geometry is shown in Fig.3. One can conclude from the dependencies in Fig.2 and Fig.3, that the both wave number and spatial resolutions are improved with antenna directivity narrowing. However it should be borne in mind that some difference between slab and cylindrical approaches appears under the large aperture of beams. The comparison of 2D plots on Fig.2c and Fig.2d points to deterioration of the both k and spatial

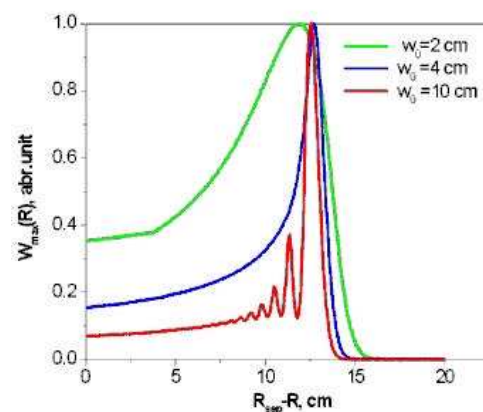


Fig.3 Normalized maxima of weighting function module versus $R-R_{sep}$ for various microwave beam radius.

resolutions for cylinder even for the ITER scale of flux surface radius. Note that all kinds of curvature influence can be accounted for with the known profile of underground plasma density. The influence of the cutoff curvature is more pronounced for small scale toroidal

devices. In Fig.4 the weighting functions for slab and cylinder approaches and the relevant detector responses are given in comparison for a small FT-2 tokamak ($R=58$ cm, $a=8$ cm). The significant broadening of 2D pattern of the detector response is clearly seen in Fig.4d. The increase of mean k -value is happened as well due to refraction effect (See Fig.4).

Summary

The 2D numerical simulation of Doppler reflectometry experiment in a case of axially symmetric distribution of plasma density proves the supported influence of antenna divergence on the k and spatial resolution [4], [5]. Under the narrow antenna directivity the curvature of flux surfaces has to be taken into account even for the large-scale fusion plasma devices. This accounting is particularly important for small tokamaks in which the flux surfaces curvature results in shift of the selected k -magnitude due to refraction and could be a reason of the scattering spectra broadening due to Doppler effect.

Acknowledgements.

This work was jointly supported by RFBR 02-02-17589 and INTAS-2001-2056.

Reference

- [1] – V.V.Bulanin, et.al, Proc. of 22nd EPS Conf. on Control. Fusion and Plasma Physics, (Bournemouth), Cont. Papers, 1995, Vol.19c, Part II, pp. 089-092.
- [2] - Zou X.L., et.al., Proc. 26th EPS Conf. on Control. Fusion and Plasma Physics (Maastricht), 1999, p.1041
- [3] – V. V. Bulanin, et.al, Plasma Physics Reports, 2000, **26**, p.813.
- [4] – Hirsch M., et.al. Plasma Phys. Control. Fusion, 2001, **43**, 1641
- [5] - E.Z.Gusakov, B.O.Yakovlev, 28th EPS Conference on Contr. Fusion and Plasma Physics (Funchal), 2001 ECA **25A**, (2001), p.361
- [6] – Novik K M and Piliya A D 1994 *Plasma Phys. Control. Fusion* **36** 357

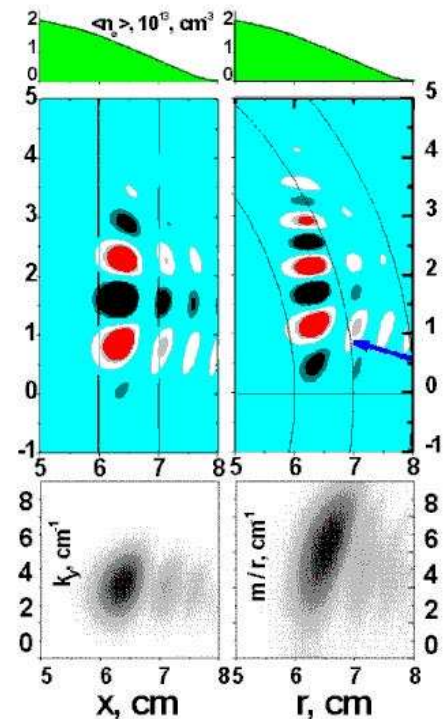


Fig.4 Comparison between slab and cylindrical approaches for Doppler reflectometry experiment in the FT-2 tokamak. $\alpha = 20^\circ$, $F=37\text{GHz}$, $w_0 = 1.5$ cm, limiter radius is 8 cm.